Direction of Arrival Estimation of Correlated Signals Using a Dynamic Linear Array

Dyonisius Dony Ariananda and Geert Leus
Faculty of EEMCS, Delft University of Technology
The Netherlands
{d.a.dyonisius, g.j.t.leus}@tudelft.nl.

***Abstract*—In this paper, we evaluate a new second-order statistics based direction of arrival (DOA) estimation method for possibly coherent sources by considering a uniform linear array (ULA) as the underlying array, and a periodic scanning where a single scanning period consists of several time slots and in different time slots, different sets of antennas in the ULA are activated leading to a dynamic array having possibly less active sensors per time slot than correlated sources. The spatial correlation matrices of the output of the antenna arrays for all time slots are collected and they can be presented as a linear function of the correlation matrix of the incoming signal at the investigated angles. Depending on the number of investigated angles, the number of time slots per scanning period, and the number of active antennas per time slot, it is possible to present our system of linear equations as an over-determined system. As long as the rank condition of the system matrix is satisfied, it is possible to first reconstruct the spatial correlation matrix of the outputs of the underlying array using LS. Given this spatial correlation matrix, we offer three alternatives. First, we can estimate the correlation matrix of the incoming signal at the investigated angles using LS. However, this option is vulnerable to a so-called grid mismatch effect. In order to mitigate this effect, we also propose structured total least-squares (S-TLS) as a second option in order to reconstruct the correlation matrix of the incoming signal at the perturbed investigated angles given the reconstructed spatial correlation matrix of the outputs of the underlying array. As a third option, we can also apply spatial smoothing and multiple signal classification (MUSIC) on the reconstructed spatial correlation matrix of the underlying array to directly obtain the DOA estimates.**

I. Introduction

We first consider a uniform linear array (ULA) having N antennas that are used to receive narrowband signals produced by K possibly correlated sources. In addition, we also assume that the wave incident on the ULA is plannar and the delay introduced between the antennas can be defined as a phase shift (due to the narrowband assumption on the incoming signals). Based on this assumption, we can write the output of the ULA at time index t as:

$$\mathbf{x}(t) = \sum_{k=1}^{K} \mathbf{a}(\theta_k) s_k(t) + \mathbf{n}(t) = \mathbf{A}\mathbf{s}(t) + \mathbf{n}(t) \quad (1)$$

where $\mathbf{x}(t)$ is the $N \times 1$ output vector containing the received signal at the N antennas of the ULA, $\mathbf{n}(t)$ is the $N \times 1$ additive noise vector, $\mathbf{s}(t) = [s_1(t), s_2(t), \ldots, s_K(t)]^T$ is the $K \times 1$ source vector with $s_k(t)$ the incoming signal from direction θ_k, and $\mathbf{A} = [\mathbf{a}(\theta_1), \mathbf{a}(\theta_2), \ldots, \mathbf{a}(\theta_K)]$ is the $N \times K$ array manifold matrix with $\mathbf{a}(\theta_k)$ the $N \times 1$ array response vector containing the phase shifts experienced by $s_k(t)$ at each element of the array. Using the first element of the ULA as a reference point, we can express the array response vector $\mathbf{a}(\theta_k)$ as

$$\mathbf{a}(\theta_k) = \left[1, a(\theta_k)^d, a(\theta_k)^{2d}, \ldots, a(\theta_k)^{(N-1)d}\right]^T \quad (2)$$

where $a(\theta_k) = \exp\left(j2\pi \sin(\theta_k)\right)$ and d is the distance in wavelengths between two consecutive antennas. In order to prevent spatial aliasing, we set d to $d \leq 0.5$. It is generally assumed that $\mathbf{n}(t)$ and $\mathbf{s}(t)$ are uncorrelated and that the impact of the wireless channel has been taken into account in $\mathbf{s}(t)$. By denoting the source correlation matrix by $\mathbf{R}_s = E[\mathbf{s}(t)\mathbf{s}^H(t)]$ and assuming that the noises at different antennas are mutually uncorrelated with variance σ_n^2, we can write the spatial correlation matrix $\mathbf{R}_x = E[\mathbf{x}(t)\mathbf{x}^H(t)]$ as

$$\mathbf{R}_x = \mathbf{A}\mathbf{R}_s\mathbf{A}^H + \sigma_n^2\mathbf{I}_N \quad (3)$$

where $\mathbf{I}_N$ is an $N \times N$ identity matrix.

Let us now introduce an antenna selection model to simulate a more general non-uniform linear array (NULA) case by activating only $M \leq N$ antennas from the discussed ULA. Starting from this point, we now refer to the considered ULA as the *underlying array*. By introducing $\mathbf{y}(t)$ as the $M \times 1$ output vector containing the output signal at the NULA of M active antennas, we can then write

$$\mathbf{y}(t) = \mathbf{C}\mathbf{x}(t) = \mathbf{C}\mathbf{A}\mathbf{s}(t) + \mathbf{C}\mathbf{n}(t) = \mathbf{B}\mathbf{s}(t) + \mathbf{C}\mathbf{n}(t) \quad (4)$$

where $\mathbf{B} = [\mathbf{b}(\theta_1), \mathbf{b}(\theta_2), \ldots, \mathbf{b}(\theta_K)]$ and $\mathbf{b}(\theta_k) = \mathbf{C}\mathbf{a}(\theta_k)$ are the $M \times K$ array manifold matrix and the $M \times 1$ array response vector, respectively, that correspond to the M activated antennas. Next, we can also write the spatial correlation matrix $\mathbf{R}_y = E[\mathbf{y}(t)\mathbf{y}^H(t)]$ as

$$\mathbf{R}_y = \mathbf{B}\mathbf{R}_s\mathbf{B}^H + \sigma_n^2\mathbf{I}_M. \quad (5)$$

Based on the NULA of M active antennas given by (4) and (5), we now introduce a number of existing DOA estimation methods.

The statistics of the incoming signals $\mathbf{s}(t)$ and the number of sources K relative to the total number of active antennas M play a major role when we review existing DOA estimation approaches. Observe that $\mathbf{R}_s$ in (5) is clearly diagonal for uncorrelated sources, is nondiagonal and full rank for partially correlated sources, and is nondiagonal and rank deficient for

fully correlated sources [1]. For uncorrelated or moderately correlated sources, it is very common to use a popular subspace based approach called MUSIC in [2] (or root-MUSIC in [3]), which exploits the eigenvalue decomposition of the spatial correlation matrix $\mathbf{R}_y$ in (5) to determine the basis for the signal and noise subspaces. Due to the full rank condition of $\mathbf{R}_s$, the noise subspace of dimension $M-K$ can be easily distinguished from the signal subspace of dimension K and hence MUSIC performs very well. Note that it is clear from the dimensions of the noise and signal subspaces that MUSIC can only estimate the DOAs of up to $K = M-1$ sources. For fully or even highly correlated signals, however, $\mathbf{R}_s$ in (5) is exactly or close to singular and theoretically, the MUSIC performance deteriorates since the dimension of the signal subspace now drops below K. This might lead to very inaccurate DOA estimates. This problem can be addressed by applying the so-called spatial smoothing preprocessing scheme discussed in [1] to $\mathbf{R}_y$ in (5) leading to a spatially smoothed covariance matrix $\overline{\mathbf{R}}_y$ that can be expressed in terms of a full rank matrix $\overline{\mathbf{R}}_s$, which is a modified version of $\mathbf{R}_s$ in (5). The MUSIC algorithm can now be applied to $\overline{\mathbf{R}}_y$ instead of $\mathbf{R}_y$. However, as mentioned in [4], the spatial smoothing scheme requires the linear array of M active antennas to have a special structure. Furthermore, the number of sources that can be detected using MUSIC after the spatial smoothing scheme usually drops to well below $K = M-1$.

A particular class of approaches, such as the ones introduced in [5] and [6], define a fine grid of investigated angles in the angular domain and then assume that the DOAs of the sources are lying at or nearby the grid points. In this case, the output of the linear array $\mathbf{y}(t)$ in (4) can be represented as

$$\mathbf{y}(t) = \sum_{q=1}^{Q} \mathbf{b}(\tilde{\theta}_q) s_{\tilde{\theta}_q}(t) + \mathbf{C}\mathbf{n}(t) = \tilde{\mathbf{B}}\tilde{\mathbf{s}}(t) + \mathbf{C}\mathbf{n}(t)$$

where $\tilde{\mathbf{s}}(t) = [s_{\tilde{\theta}_1}(t), s_{\tilde{\theta}_2}(t), \ldots, s_{\tilde{\theta}_Q}(t)]^T$ with $s_{\tilde{\theta}_q}(t)$ the unknown incident signal at the investigated angle $\tilde{\theta}_q$, and $\tilde{\mathbf{B}}$ is the $M \times Q$ array manifold matrix at the investigated angles $\{\tilde{\theta}_q\}_{q=1}^{Q}$ given by $\tilde{\mathbf{B}} = [\mathbf{b}(\tilde{\theta}_1), \mathbf{b}(\tilde{\theta}_2), \ldots, \mathbf{b}(\tilde{\theta}_Q)]$. Note that $\{\tilde{\theta}_q\}_{q=1}^{Q}$ is not necessarily the same as the set of actual angles of arrival $\{\theta_k\}_{k=1}^{K}$ contained in $\mathbf{B}$ in (4), which is not known by the receiver. Both [5] and [6] assume that $Q \gg M$ leading to $\tilde{\mathbf{B}}$ having more columns than rows. As a result, the columns of $\tilde{\mathbf{B}}$ can be regarded as an overcomplete basis for $\mathbf{y}(t)$. Under the assumption that the DOAs are constant within a certain period of time, [5] and [6] exploit multiple measurement vectors (MMVs) by collecting samples at different time indices. Hence, their data model can now be expressed as $\mathbf{Y} = \tilde{\mathbf{B}}\tilde{\mathbf{S}} + \mathbf{C}\mathbf{N}$, where $\mathbf{Y}$, $\tilde{\mathbf{S}}$, and $\mathbf{N}$ cascade $\mathbf{y}(t)$, $\tilde{\mathbf{s}}(t)$, and $\mathbf{n}(t)$, respectively, over different time indices in a row-wise fashion. By assuming that the coefficient vectors with respect to the overcomplete basis provided by the columns of $\tilde{\mathbf{B}}$ are sparse, [5] and [6] employ the so-called ℓ_1 singular value decomposition (ℓ_1-SVD) and joint ℓ_0 approximation (JLZA) algorithm, respectively, to exploit the group sparsity of the columns of $\tilde{\mathbf{S}}$ in order to identify which investigated angles are occupied by the sources.

The grid based method proposed in [7] defines the correlation matrix of the unknown incident signals at the investigated angles as $\mathbf{R}_{\tilde{s}} = E[\tilde{\mathbf{s}}(t)\tilde{\mathbf{s}}^H(t)]$ and expresses $\mathbf{R}_y$ in (5) as

$$\mathbf{R}_y = \tilde{\mathbf{B}}\mathbf{R}_{\tilde{s}}\tilde{\mathbf{B}}^H + \sigma_n^2\mathbf{I}_M. \tag{6}$$

Here, it is again assumed that $Q \gg M$, which means that the columns of $\tilde{\mathbf{B}}$ now play the role of an overcomplete basis for each column of $\mathbf{R}_y$. By again assuming that the coefficient vectors with respect to this overcomplete basis are sparse, [7] employs the ℓ_1 sparse representation of array covariance vectors (ℓ_1-SRACV) algorithm to exploit the group sparsity in the columns of $\mathbf{R}_{\tilde{s}}\tilde{\mathbf{B}}^H$ in order to locate the investigated angles occupied by the sources. It is important to note that the ℓ_1-SRACV as well as the aforementioned ℓ_1-SVD and JLZA algorithms are clearly robust to the correlation of the sources.

While the aforementioned grid-based methods and MUSIC algorithms (with spatial smoothing) can generally handle highly correlated sources, they usually require the number of active sensors M to be larger than the number of sources K. For uncorrelated sources, however, some methods have been proposed to handle more sources than physical sensors. One possible way is to exploit the fact that $\mathbf{R}_s$ in (5) is a diagonal matrix for uncorrelated sources and to express (5) as

$$\text{vec}(\mathbf{R}_y) = (\mathbf{B}^* \odot \mathbf{B})\text{diag}(\mathbf{R}_s) + \sigma_n^2\text{vec}(\mathbf{I}_M) \tag{7}$$

where vec(.) is the operator that stacks all column of a matrix into a large column vector and $\odot$ represents the Khatri-Rao product operation. The N_v distinct rows of $\mathbf{B}^* \odot \mathbf{B}$ represent the array manifold matrix of a virtual array receiving K virtual sources at K different angles. Note that the length of the virtual array, which is N_v, is generally longer than that of the original array, which is M, and it can go up to $N_v = M^2 - M + 1$. In [8], the sources are assumed to be quasi-stationary and thus diag($\mathbf{R}_s$) in (7) is generally time-varying and it only remains static over short periods of time. Due to this fact, [8] can create independent MMVs from the values of vec($\mathbf{R}_y$) in (7) obtained at different time indices, extract the basis for the noise subspace from these measurements, and estimate the DOAs using MUSIC. The exact procedure can be found in [8]. Unfortunately, when the signal is stationary, it is obvious that (7) yields a virtual array receiving a fully coherent signal since diag($\mathbf{R}_s$) is generally constant. Possible solutions are the gridding approaches of [12] and [13], or spatial smoothing and MUSIC [9], [10], [11]. Note that the latter requires a uniform virtual array, which can be obtained by introducing a special array design of M antennas such as a two-level nested array [9], a coprime array [10], [11] or a sparse ruler array [12].

All the aforementioned methods either focus on correlated sources or on more sources than sensors but not on both of them. There is actually an approach that tried to tackle more correlated sources than sensors, i.e., the one proposed in [14]. However, this approach involves the computation of fourth-order statistics leading to a higher level of computational complexity. Therefore, our focus in this paper is on how to design a DOA estimation method that is able to handle more

highly correlated sources than active sensors and that involves the computation of at most second-order statistics.

II. Dynamic Linear Array via Periodic Scanning

In order to estimate the DOAs of possibly correlated or even fully coherent sources using less active antennas than sources, we propose a novel dynamic linear array, which also uses the ULA of N antennas introduced in (1) as the underlying array. In general, we activate only M out of N available antennas in the ULA within a specific time slot where the set of M activated antennas in different time slots can be different. While the number of required physical antennas is still equal to N, the number of hardware receiver branches can be reduced from N to M leading to a smaller power consumption while maintaining the ability to locate the DOAs of the incoming correlated signals. It is also possible to employ only $M < N$ movable physical antennas to construct a dynamic linear array. In this case, it is assumed that the position of each antenna in different time slots can be altered.

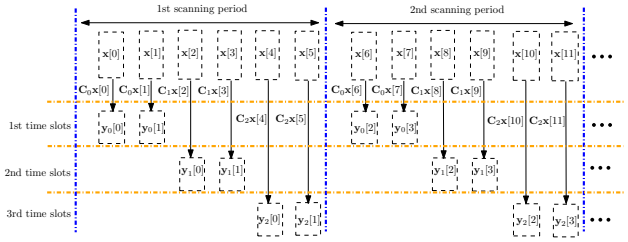

Fig. 1. Illustration of the periodic scanning process where a single scanning period consists of L time slots. In this example, $L = 3$ and the number of samples per slot in every antenna is equal to $S = 2$

Let us first consider the ULA model provided by (1) and recall that $\mathbf{x}(t)$ is the output vector of the N antennas in the ULA. We introduce $\mathbf{x}[n]$ as a digital representation of $\mathbf{x}(t)$, i.e., $\mathbf{x}[n] = \mathbf{x}(nT)$ where T is the sampling time at every analog-to-digital converter (ADC) associated with each antenna. For simplicity, we assume that the sampling rate $1/T$ is the same for all ADCs. Next, let us focus on the periodic scanning described in Fig. 1 using the considered ULA model where a single scanning period consists of L time slots. In different time slots of a certain scanning period, different sets of M antennas are activated out of N available antennas while the set of M active antennas in the l-th time slot of different scanning periods is the same. Denote the number of received samples per antenna within one time slot by S and the total number of scanning periods by P. We then introduce $\mathbf{y}_l[m]$ as the $M \times 1$ vector representing the outputs of the M active antennas in the array in the l-th time slot, which is given by:

$$\mathbf{y}_l[pS + s] = \mathbf{C}_l \mathbf{x}[(pL + l)S + s] \text{ for } l = 0, 1, \ldots, L-1,$$

where the $M \times N$ matrix $\mathbf{C}_l$ is formed by selecting M out of N rows from the identity matrix $\mathbf{I}_N$, $s = 0, 1, \ldots, S-1$, and $p = 0, 1, \ldots, P-1$. Note that the indices of the M selected rows represent the indices of the M active antennas in the l-th time slot selected from N available antennas in the ULA. By taking into account the fact that $\mathbf{C}_l$ is a real matrix, the $M \times M$ spatial correlation matrix of $\mathbf{y}_l[m]$ is then given by

$$\begin{aligned} \mathbf{R}_{y_l} &= E\left[\mathbf{y}_l[m]\mathbf{y}_l[m]^H\right] = \mathbf{C}_l \mathbf{R}_x \mathbf{C}_l^T \\ &= \mathbf{C}_l \mathbf{A} \mathbf{R}_s \mathbf{A}^H \mathbf{C}_l^T + \sigma_n^2 \mathbf{I}_M. \end{aligned} \tag{8}$$

In practice, the expectation operation in (8) can be estimated by taking an average over PS time samples. After stacking all columns of $\mathbf{R}_{y_l}$ into the $M^2 \times 1$ vector $\text{vec}(\mathbf{R}_{y_l})$, we can then express $\text{vec}(\mathbf{R}_{y_l})$ using (8) as

$$\mathbf{r}_{y_l} = \text{vec}(\mathbf{R}_{y_l}) = (\mathbf{C}_l \otimes \mathbf{C}_l)\text{vec}(\mathbf{R}_x) \tag{9}$$

where $\otimes$ denotes the Kronecker product operation. We can eventually combine $\mathbf{r}_{y_l}$ in (9) for all time slots into a single vector $\mathbf{r}_y$ given by $\mathbf{r}_y = \left[\mathbf{r}_{y_0}^T, \mathbf{r}_{y_1}^T, \ldots, \mathbf{r}_{y_{L-1}}^T\right]^T$. The relationship between $\mathbf{r}_y$ and $\mathbf{R}_x$ in (9) is then written as

$$\mathbf{r}_y = \mathbf{\Psi}\text{vec}(\mathbf{R}_x) \tag{10}$$

where the $M^2 L \times N^2$ matrix $\mathbf{\Psi}$ is given by

$$\mathbf{\Psi} = \left[(\mathbf{C}_0 \otimes \mathbf{C}_0)^T, (\mathbf{C}_1 \otimes \mathbf{C}_1)^T, \ldots, (\mathbf{C}_{L-1} \otimes \mathbf{C}_{L-1})^T\right]^T. \tag{11}$$

Our first step is to reconstruct $\text{vec}(\mathbf{R}_x)$ from $\mathbf{r}_y$ in (10) using least squares (LS), which is only possible if $M^2 L \geq N^2$ and $\mathbf{\Psi}$ in (11) has full column rank. Recall that $M < N$, which means that $M^2 L \geq N^2$ only if $L \geq 2$. This is equal to saying that a dynamic linear array via periodic scanning is necessary to recover $\text{vec}(\mathbf{R}_x)$ from $\mathbf{r}_y$. When $\mathbf{\Psi}$ in (11) has full column rank, we obtain

$$\text{vec}(\hat{\mathbf{R}}_x) = (\mathbf{\Psi}^T \mathbf{\Psi})^{-1} \mathbf{\Psi}^T \mathbf{r}_y. \tag{12}$$

Let us now consider the following lemma.

Lemma 1: $\mathbf{C}_l \otimes \mathbf{C}_l$ will have a one in the $[(i-1)N + j]$-th and $[(j-1)N + i]$-th columns if and only if $\mathbf{C}_l$ contains the i-th and j-th rows of the identity matrix $\mathbf{I}_N$.

The following corollary directly follows from Lemma 1.

Corollary 1: If we select M different rows of $\mathbf{I}_N$ to form $\mathbf{C}_l$, the rows of $\mathbf{C}_l \otimes \mathbf{C}_l$ have a single one at exactly M^2 different positions. Out of the M^2 rows of $\mathbf{C}_l \otimes \mathbf{C}_l$, M rows are produced by the self-Kronecker product of every row of $\mathbf{C}_l$. In addition, every pair of two different rows of $\mathbf{C}_l$ contributes to two different rows of $\mathbf{C}_l \otimes \mathbf{C}_l$, each of which has a single one at a different position. Since we have $\binom{M}{2}$ possible combinations of two different rows, all Kronecker products between any two different rows of $\mathbf{C}_l$ lead to $M(M-1)$ rows of $\mathbf{C}_l \otimes \mathbf{C}_l$, all of which have a single one at a different position.

We define Γ_l as the set of M indices selected from $\{1, 2, \ldots, N\}$ representing the rows of $\mathbf{I}_N$ that we use to construct $\mathbf{C}_l$. The indices of the columns of $\mathbf{C}_l \otimes \mathbf{C}_l$ that contain a one are then provided by Ω_l, which is the set given by:

$$\Omega_l = \{(i-1)N + j | \forall i, j \in \Gamma_l\}. \tag{13}$$

From (11) and the fact that each row of $\mathbf{C}_l \otimes \mathbf{C}_l$ has only a single one, it is obvious that every row of $\mathbf{\Psi}$ also has only a single one. Therefore, the full column rank condition of $\mathbf{\Psi}$ is achieved if each of its columns has at least a single one. Our task now is to construct $\{\mathbf{C}_l\}_{l=0}^{L-1}$ subject to the full column

rank condition of $\mathbf{\Psi}$ in (10). From (11) and (13), it is clear that this can be achieved if and only if

$$\bigcup_{l=0}^{L-1} \Omega_l = \left\{1, 2, \ldots, N^2\right\}. \tag{14}$$

Our aim is to achieve (14) in order to ensure the full column rank condition of $\mathbf{\Psi}$ while keeping the number of active antennas and hardware receiver branches M small, the number of antenna reconfigurations per scanning period L minimal, and the computational complexity low. Unfortunately, it is not possible to simultaneously minimize the aforementioned variables. For example, let us focus on the system matrix $\mathbf{\Psi}$ in (11). Since Corrolary 1 indicates that, for a given $l \in \{0, 1, \ldots, L-1\}$, only M^2 out of N^2 columns of $\mathbf{C}_l \otimes \mathbf{C}_l$ have at least a single one, minimizing M results in a smaller number of columns of $\mathbf{C}_l \otimes \mathbf{C}_l$ having a one. Consequently, we need a larger L to ensure that every column of $\mathbf{\Psi}$ has at least a single one. In other words, it is impossible to simultaneously minimize L and M. Also, observe that the number of rows of $\mathbf{\Psi}$ in (10) to be inverted, which determines the computational complexity, depends quadratically on M and linearly on L.

TABLE I
ALGORITHM 1: A GREEDY ALGORITHM TO FIND A SUB-OPTIMAL SOLUTION FOR L AND $\{\Gamma_l\}_{l=0}^{L-1}$ GIVEN M SUBJECT TO (14).

Algorithm 1	
1:	Introduce $\mathbf{Z}^{(f)}$ as an $N \times N$ indicator matrix at the f-th iteration and denote its element at the i-th row and the j-th column by $\left[\mathbf{Z}^{(f)}\right]_{i,j}$.
2:	Initialize $f = 0$ and $\mathbf{Z}^{(0)} = \mathbf{I}_N$.
3:	While $\mathbf{Z}^{(f)}$ has at least one zero entry do
4:	Set $f = f + 1$ and $\mathbf{Z}^{(f)} = \mathbf{Z}^{(f-1)}$.
5:	Randomly select $i, j \in \{1, 2, \ldots, N\}$ for which $\left[\mathbf{Z}^{(f)}\right]_{i,j} = 0$ and set $\Gamma_{f-1} = \{i, j\}$. Then also set both $\left[\mathbf{Z}^{(f)}\right]_{i,j}$ and $\left[\mathbf{Z}^{(f)}\right]_{j,i}$ to 1.
6:	for $\kappa = 1$ to $M - 2$ do
7:	Define a set $\Xi = \{1, 2, \ldots, N\} \setminus \Gamma_{f-1}$.
8:	Search in Ξ for the element g that satisfies: $g = \arg\min_{g' \in \Xi} \sum_{i' \in \Gamma_{f-1}} \left[\mathbf{Z}^{(f)}\right]_{i',g'}$.
9:	For all $i' \in \Gamma_{f-1}$ set $\left[\mathbf{Z}^{(f)}\right]_{i',g}$ and $\left[\mathbf{Z}^{(f)}\right]_{g,i'}$ to 1.
10:	Update Γ_{f-1} to $\Gamma_{f-1} = \Gamma_{f-1} \bigcup \{g\}$.
11:	end for
12:	end while
13:	The value of L is given by $L = f$ and the output of this algorithm is $\{\Gamma_l\}_{l=0}^{L-1}$.

It is obvious from Corollary 1 and Lemma 1 that two conditions have to be satisfied in order to ensure the full column rank condition of $\mathbf{\Psi}$. First of all, each row of $\mathbf{I}_N$ should be used to construct at least one of the L possible matrices $\{\mathbf{C}_l\}_{l=0}^{L-1}$. According to Lemma 1 and Corollary 1, this will ensure that the $(i-1)N+i$-th column of $\mathbf{\Psi}$ has at least a single one for all $i \in \{1, \ldots, N\}$. This first condition also implies that every antenna out of N available antennas provided by the ULA in (1) should be active in at least one time slot within every scanning period. Secondly, every possible pair of two different rows of $\mathbf{I}_N$ should be used in at least one of the L possible matrices $\{\mathbf{C}_l\}_{l=0}^{L-1}$ in order to ensure that the $(i-1)N + j$-th and the $(j-1)N + i$-th columns of $\mathbf{\Psi}$ have at least a single one for all $i \neq j$ and $i, j \in \{1, \ldots, N\}$. As a consequence, each possible combination of two antennas in the ULA should be active in at least one of the L possible time slots within a single scanning period, which also means that $M \geq 2$ is automatically required. Since the second condition requires every antenna in the ULA to be active in at least one time slot, satisfying the second condition automatically guarantees the first condition.

TABLE II
ALGORITHM 2: A GREEDY ALGORITHM TO FIND A SUB-OPTIMAL SOLUTION FOR M AND $\{\Gamma_l\}_{l=0}^{L-1}$ GIVEN L SUBJECT TO (14)

Algorithm 2	
1:	Introduce $\mathbf{Z}^{(f)}$ as an $N \times N$ indicator matrix at the f-th iteration and denote its element at the i-th row and the j-th column by $\left[\mathbf{Z}^{(f)}\right]_{i,j}$.
2:	Initialize $f = 0$ and $\mathbf{Z}^{(0)} = \mathbf{I}_N$.
3:	Set $f = f + 1$ and $\mathbf{Z}^{(f)} = \mathbf{Z}^{(f-1)}$.
4:	for $l = 0$ to $L - 1$ do
5:	Randomly select $i, j \in \{1, 2, \ldots, N\}$ for which $\left[\mathbf{Z}^{(f)}\right]_{i,j} = 0$ and set $\Gamma_l = \{i, j\}$.
6:	Set both $\left[\mathbf{Z}^{(f)}\right]_{i,j}$ and $\left[\mathbf{Z}^{(f)}\right]_{j,i}$ to 1.
7:	end for
8:	While $\mathbf{Z}^{(f)}$ has at least one zero entry do
9:	Set $f = f + 1$ and then set $\mathbf{Z}^{(f)} = \mathbf{Z}^{(f-1)}$.
10:	for $\kappa = 0$ to $L - 1$ do
11:	Define a set $\Xi = \{1, 2, \ldots, N\} \setminus \Gamma_\kappa$.
12:	Search in Ξ for the element g that satisfies: $g = \arg\min_{g' \in \Xi} \sum_{i' \in \Gamma_\kappa} \left[\mathbf{Z}^{(f)}\right]_{i',g'}$.
13:	For all $i' \in \Gamma_\kappa$ set $\left[\mathbf{Z}^{(f)}\right]_{i',g}$ and $\left[\mathbf{Z}^{(f)}\right]_{g,i'}$ to 1.
14:	Update Γ_κ to $\Gamma_\kappa = \Gamma_\kappa \bigcup \{g\}$.
15:	end for
16:	end while
17:	The value of M is given by $M = f + 1$ and the output of this algorithm is $\{\Gamma_l\}_{l=0}^{L-1}$.

Subject to (14), we now try to minimize L given M. Let us first introduce Λ as $\Lambda = \{(i,j) | i, j \in \{1, 2, \ldots, N\}, i < j\}$ and Λ_l as the set of all possible combinations of two row indices of $\mathbf{I}_N$ that are used to construct $\mathbf{C}_l$, that is $\Lambda_l = \{(i,j) | i, j \in \Gamma_l, i < j\}$. We can then write the problem of minimizing L given $M \geq 2$ subject to (14) as

$$\min_{\{\Gamma_l\}_{l=0}^{L-1}} L \text{ subject to } \bigcup_{l=0}^{L-1} \Lambda_l = \Lambda \text{ and } |\Gamma_l| = M, \forall l \tag{15}$$

where $|\Gamma_l|$ denotes the cardinality of the set Γ_l. While the minimization problem in (15) is generally a non-trivial combinatorial problem, a lower bound for L can be found. Due to the fact that $|\Lambda| = N(N-1)/2$ and $|\Lambda_l| = M(M-1)/2$, L is lower bounded by

$$L \geq \left\lceil \frac{|\Lambda|}{|\Lambda_l|} \right\rceil = \left\lceil \frac{N(N-1)}{M(M-1)} \right\rceil \tag{16}$$

where $\lceil x \rceil$ represents the smallest integer not smaller than x. Since it is not trivial to find a closed-form solution for the problem in (15), we propose a greedy algorithm to find a sub-optimal solution for L and $\{\Gamma_l\}_{l=0}^{L-1}$ given M subject to (14). This algorithm is described in Table I. The indicator matrix $\mathbf{Z}^{(f)}$ in Table I is used to indicate whether a particular combination of two antennas has been used in the first f time slots. For example, if a combination of the i-th and the j-th antennas has never been simultaneously used in the first f time slots, then $[\mathbf{Z}^{(f)}]_{i,j} = 0$. On the other hand, $[\mathbf{Z}^{(f)}]_{i,j} = 1$

implies that the combination of the i-th and the j-th antennas has been simultaneously used at least once in the first f time slots. It is also clear that $\mathbf{Z}^{(f)}$ is a symmetric matrix. Recall that our goal is to ensure that each possible combination of two antennas in the ULA is active in at least one of the L possible time slots within a scanning period. As a result, we initialize $\mathbf{Z}^{(f)}$ with $\mathbf{Z}^{(0)} = \mathbf{I}_N$ since we are only interested in the off-diagonal components of $\mathbf{Z}^{(f)}$. The goal of the while loop in Table I is to select M antennas for every time slot. First, we randomly select a combination of two antennas that has not been used in the previous time slot. This is indicated by step 5 in Table I. The inner for loop in Table I aims to select the remaining $M-2$ antennas for the considered time slot. Here, for every antenna selection, the goal is to maximize the number of conversion of zeros in $\mathbf{Z}^{(f)}$ to ones. In other words, we want to ensure that every antenna selection results in a maximum number of new combinations of two active antennas that have not been simultaneously activated in the previous time slots.

Similarly, we can also express the minimization of M subject to (14) given L as

$$\min_{\{\Gamma_l\}_{l=0}^{L-1}} M \text{ subject to } \bigcup_{l=0}^{L-1} \Lambda_l = \Lambda \text{ and } |\Gamma_l| = M, \forall l.$$

The lower bound for M is then given by

$$\frac{M^2 - M}{2} \geq \left\lceil \frac{|\Lambda|}{L} \right\rceil = \left\lceil \frac{N(N-1)}{2L} \right\rceil. \tag{17}$$

Table II illustrates the proposed greedy algorithm to find a sub-optimal solution for M and $\{\Gamma_l\}_{l=0}^{L-1}$ given L subject to (14). The notation used by Algorithm 2 in Table II is similar to the one used by Algorithm 1. However, we now consider all time slots simultaneously and thus $\mathbf{Z}^{(f)}$ is now used to indicate whether a particular combination of two antennas has been used in the first $f+1$ antennas in any time slot. The first for loop in Algorithm 2 is used to select the first two antennas in every time slot. Next, every iteration of the while loop (see steps 8-16) selects one additional antenna for all time slots. Similar to Algorithm 1, every antenna selection aims to maximize the number of conversion of zeros in $\mathbf{Z}^{(f)}$ to ones.

III. Signal Correlation Recovery and Direction of Arrival Estimation

A. Least Squares Approach

Once $\mathbf{R}_x$ is reconstructed from (10) using LS, we can then proceed to DOA estimation. One possible way is to define a fine grid of investigated angles in the angular domain, and use a model similar to (6), but now applied to the underlying ULA. In other words, based also on (3), we can write $\mathbf{R}_x$ as

$$\text{vec}\,(\mathbf{R}_x) = (\tilde{\mathbf{A}}^* \otimes \tilde{\mathbf{A}})\text{vec}\,(\mathbf{R}_{\tilde{s}}) + \sigma_n^2 \text{vec}\,(\mathbf{I}_N) \tag{18}$$

where $\tilde{\mathbf{A}}$ is the $N \times Q$ array response matrix of the underlying ULA at the investigated angles $\{\tilde{\theta}_q\}_{q=1}^{Q}$ given by $\tilde{\mathbf{A}} = [\mathbf{a}(\tilde{\theta}_\mathbf{1}), \mathbf{a}(\tilde{\theta}_\mathbf{2}), \ldots, \mathbf{a}(\tilde{\theta}_\mathbf{Q})]$. Based on (18), $\text{vec}\,(\mathbf{R}_{\tilde{s}})$ can be reconstructed from $\text{vec}(\mathbf{R}_x)$ using LS as long as $\tilde{\mathbf{A}}$ has full column rank, which is only possible if $Q \leq N$. In this case, we can solve (18) as

$$\text{vec}(\hat{\mathbf{R}}_{\tilde{s}}) = ((\tilde{\mathbf{A}}^* \otimes \tilde{\mathbf{A}})^H (\tilde{\mathbf{A}}^* \otimes \tilde{\mathbf{A}}))^{-1} (\tilde{\mathbf{A}}^* \otimes \tilde{\mathbf{A}})^H \text{vec}\,(\mathbf{R}_x).$$

Since the full column rank condition of $\tilde{\mathbf{A}}$ has to be guaranteed, the selection of the investigated angles $\tilde{\theta}_q$ is not arbitrary although we can generally compute $\hat{\mathbf{R}}_{\tilde{s}}$ for up to N investigated angles $\tilde{\theta}_q$. One easy option is to use a half wavelength spacing in the underlying ULA by setting d in (2) to $d = 0.5$ and use an inverse sinusoidal grid for $\{\tilde{\theta}_q\}_{q=1}^{Q}$, i.e.,

$$\tilde{\theta}_q = \sin^{-1}\left(\frac{2}{Q}\left(q - 1 - \left\lceil \frac{Q-1}{2} \right\rceil\right)\right) \tag{19}$$

for $q = 1, 2, \ldots, Q$. When we set $d = 0.5$, $Q = N$ and $\{\tilde{\theta}_q\}_{q=1}^{Q}$ according to (19), we can easily find that $\tilde{\mathbf{A}}$ is a permuted version of the inverse discrete Fourier transform (IDFT) matrix, which means that applying the inverse of $\tilde{\mathbf{A}}^* \otimes \tilde{\mathbf{A}}$ to $\text{vec}(\mathbf{R}_x)$ in (18) can easily be performed using the fast Fourier transform (FFT).

Once $\hat{\mathbf{R}}_{\tilde{s}}$ is computed, we can find that its diagonal components contain the received power at the investigated angles $\{\tilde{\theta}_q\}_{q=1}^{Q}$, and thus we can consider $\text{diag}(\hat{\mathbf{R}}_{\tilde{s}})$ as an angular spectrum. Next, we can find the estimates of the actual DOAs by locating the peaks of this spectrum. Meanwhile, the off-diagonal components of $\hat{\mathbf{R}}_{\tilde{s}}$ contain the correlation between the signals received at the different investigated angles. If we want to estimate the angles at a larger resolution we have to take $Q > N$ and adopt a sparsity constraint (possibly assisted by a positivity constraint) as done in [13]. However, for non-sparse angular spectra, this approach is not viable.

B. Structured Total Least Squares

When the DOA of a particular source k is not exactly the same as any of the defined investigated angles, i.e., $\theta_k \neq \tilde{\theta}_q$ for $q = 1, 2, \ldots, Q$, a so-called grid mismatch effect is introduced. If the error introduced by the grid mismatch effect is significant, the performance of the LS estimate in Section III-A deteriorates. Let us now take into account this grid mismatch effect by introducing a kind of unknown additive error or perturbation δ_q on the investigated angle $\tilde{\theta}_q$. Consequently, the corresponding array response vector is given by $\mathbf{a}(\tilde{\theta}_q + \delta_q) = [1, a(\tilde{\theta}_q + \delta_q)^d, a(\tilde{\theta}_q + \delta_q)^{2d}, \ldots, a(\tilde{\theta}_q + \delta_q)^{(N-1)d}]^T$. Under the assumption that the perturbation δ_q is sufficiently small, $a(\tilde{\theta}_q + \delta_q)^{nd}$ can be interpolated using a first-order Taylor series around $\tilde{\theta}_q$ as:

$$a(\tilde{\theta}_q + \delta_q)^{nd} \approx a(\tilde{\theta}_q)^{nd} + \left(\partial(a(\tilde{\theta})^{nd})/\partial\tilde{\theta}\right)\Big|_{\tilde{\theta}=\tilde{\theta}_q} \delta_q, \tag{20}$$

for $n = 0, 1, \ldots, N-1$ and $q = 1, 2, \ldots, Q$. Next, let us collect the right-hand side values of the approximation in (20) for all n and q, and stack them in the matrix

$$\check{\mathbf{A}} = \tilde{\mathbf{A}} + \tilde{\mathbf{A}}' \text{diag}(\boldsymbol{\delta}) \tag{21}$$

where $\boldsymbol{\delta} = [\delta_1, \delta_2, \ldots, \delta_Q]^T$ and $\tilde{\mathbf{A}}'$ is given by $\tilde{\mathbf{A}}' = [\mathbf{a}'(\tilde{\theta}_1), \mathbf{a}'(\tilde{\theta}_2), \ldots, \mathbf{a}'(\tilde{\theta}_Q)]$ with $\mathbf{a}'(\tilde{\theta}_q)$ provided by

$$\mathbf{a}'(\tilde{\theta}_q) = \left[0, \left.\frac{\partial(a(\tilde{\theta})^d)}{\partial\tilde{\theta}}\right|_{\tilde{\theta}=\tilde{\theta}_q}, \ldots, \left.\frac{\partial(a(\tilde{\theta})^{(N-1)d})}{\partial\tilde{\theta}}\right|_{\tilde{\theta}=\tilde{\theta}_q}\right]^T.$$

As a result, we can rewrite our problem (18) as

$$\text{vec}\,(\mathbf{R}_x) = (\check{\mathbf{A}}^* \otimes \check{\mathbf{A}})\text{vec}\,(\mathbf{R}_{\check{s}}) + \sigma_n^2 \text{vec}\,(\mathbf{I}_N) \tag{22}$$

where $\mathbf{R}_{\check{s}}$ is the correlation matrix of the unknown incident signals at the perturbed investigated angles $\{\tilde{\theta}_q + \delta_q\}_{q=1}^{Q}$. Using (21) and the fact that $\text{diag}(\boldsymbol{\delta})$ is a real matrix, we can rewrite (22) as

$$\begin{aligned}
&\text{vec}\,(\mathbf{R}_x) = [\tilde{\mathbf{A}}^* \otimes \tilde{\mathbf{A}} + (\tilde{\mathbf{A}}'^* \otimes \tilde{\mathbf{A}})(\text{diag}(\boldsymbol{\delta}) \otimes \mathbf{I}_Q) \\
&+ (\tilde{\mathbf{A}}^* \otimes \tilde{\mathbf{A}}')(\mathbf{I}_Q \otimes \text{diag}(\boldsymbol{\delta})) + (\tilde{\mathbf{A}}'^* \otimes \tilde{\mathbf{A}}') \times \\
&(\text{diag}(\boldsymbol{\delta}) \otimes \text{diag}(\boldsymbol{\delta}))]\text{vec}\,(\mathbf{R}_{\check{s}}) + \sigma_n^2 \text{vec}\,(\mathbf{I}_N) \\
&\approx [\tilde{\mathbf{A}}^* \otimes \tilde{\mathbf{A}} + (\tilde{\mathbf{A}}'^* \otimes \tilde{\mathbf{A}})(\text{diag}(\boldsymbol{\delta}) \otimes \mathbf{I}_Q) \\
&+ (\tilde{\mathbf{A}}^* \otimes \tilde{\mathbf{A}}')(\mathbf{I}_Q \otimes \text{diag}(\boldsymbol{\delta}))]\text{vec}\,(\mathbf{R}_{\check{s}}) + \sigma_n^2 \text{vec}\,(\mathbf{I}_N) \\
&= (\tilde{\mathbf{A}}^* \otimes \tilde{\mathbf{A}} + \mathbf{E}(\boldsymbol{\delta}))\text{vec}\,(\mathbf{R}_{\check{s}}) + \sigma_n^2 \text{vec}\,(\mathbf{I}_N)
\end{aligned} \tag{23}$$

where $\mathbf{E}(\boldsymbol{\delta}) = (\tilde{\mathbf{A}}'^* \otimes \tilde{\mathbf{A}})(\text{diag}(\boldsymbol{\delta}) \otimes \mathbf{I}_Q) + (\tilde{\mathbf{A}}^* \otimes \tilde{\mathbf{A}}')(\mathbf{I}_Q \otimes \text{diag}(\boldsymbol{\delta}))$ is introduced to simplify the writing and the approximation is based on the assumption that $\text{diag}(\boldsymbol{\delta}) \otimes \text{diag}(\boldsymbol{\delta})$ is negligible, which is due to the assumption that δ_q is sufficiently small. Comparing (23) with (18), we can view (23) as a structured total least squares (S-TLS) problem where $\mathbf{E}(\boldsymbol{\delta})$ is perceived as a perturbation matrix for $\tilde{\mathbf{A}}^* \otimes \tilde{\mathbf{A}}$ and $\sigma_n^2 \text{vec}\,(\mathbf{I}_N)$ is regarded as a deterministic error on $\text{vec}\,(\mathbf{R}_x)$.

Based on (23), our goal is to solve the following minimization problem

$$\min_{\boldsymbol{\delta}, \text{vec}(\mathbf{R}_{\check{s}})} \|\boldsymbol{\delta}\|_2^2 + \|\text{vec}\,(\mathbf{R}_x) - (\tilde{\mathbf{A}}^* \otimes \tilde{\mathbf{A}} + \mathbf{E}(\boldsymbol{\delta}))\text{vec}\,(\mathbf{R}_{\check{s}})\,\|_2^2. \tag{24}$$

One easy way to solve (24) is to use an alternating descent algorithm. When $\boldsymbol{\delta}$ is available, the minimization problem in (24) is reduced to an ordinary LS problem and we can solve $\text{vec}\,(\mathbf{R}_{\check{s}})$ directly from (23) using LS. Next, let us introduce $\mathbf{1}_{Q\times Q}$ as a $Q \times Q$ matrix with all entries equal to one. When $\text{vec}(\mathbf{R}_{\check{s}})$ is available, we can use $\text{diag}(\text{diag}(\boldsymbol{\delta}) \otimes \mathbf{I}_Q) = (\mathbf{I}_Q \odot \mathbf{1}_{Q\times Q})\boldsymbol{\delta}$ and $\text{diag}(\mathbf{I}_Q \otimes \text{diag}(\boldsymbol{\delta})) = (\mathbf{1}_{Q\times Q} \odot \mathbf{I}_Q)\boldsymbol{\delta}$ to rewrite (23) as

$$\begin{aligned}
&\text{vec}\,(\mathbf{R}_x) - \sigma_n^2 \text{vec}\,(\mathbf{I}_N) = (\tilde{\mathbf{A}}^* \otimes \tilde{\mathbf{A}})\text{vec}\,(\mathbf{R}_{\check{s}}) \\
&+ \Big((\tilde{\mathbf{A}}'^* \otimes \tilde{\mathbf{A}})\text{diag}(\text{vec}\,(\mathbf{R}_{\check{s}}))(\mathbf{I}_Q \odot \mathbf{1}_{Q\times Q}) \\
&+ (\tilde{\mathbf{A}}^* \otimes \tilde{\mathbf{A}}')\text{diag}(\text{vec}\,(\mathbf{R}_{\check{s}}))(\mathbf{1}_{Q\times Q} \odot \mathbf{I}_Q)\Big)\,\boldsymbol{\delta} \\
&= \mathbf{w} + \boldsymbol{\Phi}\boldsymbol{\delta}
\end{aligned} \tag{25}$$

where $\boldsymbol{\Phi} = (\tilde{\mathbf{A}}'^* \otimes \tilde{\mathbf{A}})\text{diag}(\text{vec}\,(\mathbf{R}_{\check{s}}))(\mathbf{I}_Q \odot \mathbf{1}_{Q\times Q}) + (\tilde{\mathbf{A}}^* \otimes \tilde{\mathbf{A}}')\text{diag}(\text{vec}\,(\mathbf{R}_{\check{s}}))(\mathbf{1}_{Q\times Q} \odot \mathbf{I}_Q)$ and $\mathbf{w} = (\tilde{\mathbf{A}}^* \otimes \tilde{\mathbf{A}})\text{vec}\,(\mathbf{R}_{\check{s}})$ are introduced to simplify the writing. The minimization problem in (24) when $\text{vec}(\mathbf{R}_{\check{s}})$ is available can then be written as:

$$\min_{\boldsymbol{\delta}} \|\boldsymbol{\delta}\|_2^2 + \|\text{vec}\,(\mathbf{R}_x) - \mathbf{w} - \boldsymbol{\Phi}\boldsymbol{\delta}\|_2^2 \tag{26}$$

which is quadratic in $\boldsymbol{\delta}$. The solution for (26) can be straightforwardly derived and it is given by

$$\hat{\boldsymbol{\delta}} = (\mathbf{I}_Q + \text{Re}(\boldsymbol{\Phi}^H\boldsymbol{\Phi}))^{-1}\text{Re}(\boldsymbol{\Phi}^H(\text{vec}(\mathbf{R}_x) - \mathbf{w})) \tag{27}$$

where Re(.) returns the real part of a complex number. The alternating descent algorithm basically performs iterations that includes solving $\text{vec}\,(\mathbf{R}_{\check{s}})$ from (23) using LS and solving (26) using (27). This algorithm is summarized in Table III.

TABLE III
THE ALTERNATING DESCENT ALGORITHM USED TO SOLVE THE S-TLS MINIMIZATION PROBLEM GIVEN BY (24).

0:	**Notation**: $\boldsymbol{\delta}(i)$ and $\text{vec}(\mathbf{R}_{\check{s}})(i)$ represent the values of $\boldsymbol{\delta}$ and $\text{vec}(\mathbf{R}_{\check{s}})$ at the i-th iteration, respectively.
1:	**Inputs**: $\tilde{\mathbf{A}}, \tilde{\mathbf{A}}', \mathbf{R}_x, \epsilon$, maxiteration.
2:	Initialize $\boldsymbol{\delta}(0) = \mathbf{0}$.
3:	Solve $\text{vec}(\mathbf{R}_{\check{s}})(0)$ from (23) using LS with $\mathbf{E}(\boldsymbol{\delta}(0)) = 0$ due to step 2.
4:	**for** $i = 1$ to maxiteration do
5:	For given $\text{vec}(\mathbf{R}_{\check{s}})(i-1)$, compute $\boldsymbol{\delta}(i)$ using (27).
6:	For given $\boldsymbol{\delta}(i)$, compute $\mathbf{E}(\boldsymbol{\delta}(i))$ and solve $\text{vec}(\mathbf{R}_{\check{s}})(i)$ from (23) using LS.
7:	**if** $\|\text{vec}(\mathbf{R}_{\check{s}})(i) - \text{vec}(\mathbf{R}_{\check{s}})(i-1)\|_2 < \epsilon$ then break.
8:	**end for**
9:	**Outputs**: $\hat{\boldsymbol{\delta}}$,$\text{vec}(\hat{\mathbf{R}}_{\check{s}})$.

Similar to Section III-A, the diagonal components of the resulting $\hat{\mathbf{R}}_{\check{s}}$ contain the received power at the perturbed investigated angles $\{\tilde{\theta}_q + \hat{\delta}_q\}_{q=1}^{Q}$. The estimates of the actual DOAs can be found by locating the peaks of the angular spectrum provided by $\text{diag}(\hat{\mathbf{R}}_{\check{s}})$. The off-diagonal components of $\hat{\mathbf{R}}_{\check{s}}$ again contain the correlation between the signals received at the different angles $\{\tilde{\theta}_q + \hat{\delta}_q\}_{q=1}^{Q}$. Note that for this algorithm to work, we need an overdetermined system, and as such we require $Q < N$. If we want to estimate the angles at a larger resolution, we can take $Q > N$ and rely on a sparsity constraint, leading to a sparse version of our S-TLS method. Deriving such an approach would follow similar steps as [15], but it goes beyond the scope of this paper. Again, such an approach would not work for estimating a non-sparse spectrum.

C. MUSIC and Spatial Smoothing

The fact that we use a ULA of N antennas as our underlying array also allows us to apply the spatial smoothing preprocessing scheme of [1] to the recovered $\hat{\mathbf{R}}_{x}$ in (12) leading to a spatially smoothed correlation matrix $\hat{\hat{\mathbf{R}}}_x$. The MUSIC algorithm in [2] can then be applied to the resulting $\hat{\hat{\mathbf{R}}}_x$ leading to high resolution DOA estimates. In our case, the underlying ULA can be divided into N_s overlapping subarrays, each of which has N_a physical antennas. Observe that having a larger N_s implies having a smaller N_a and vise versa. Also notice that the maximum number of sources that can be detected by MUSIC after the spatial smoothing process is equal to $\min(N_s, N_a - 1)$ [1]. As a result, it is important to find the optimum values for N_s and N_a, i.e., the ones that lead to the largest possible number of sources that can be detected. In the case of our underlying ULA, it can be shown that the optimum value for N_s is given by $N_s = \lceil \frac{N}{2} \rceil$.

IV. NUMERICAL STUDY

In this section, the proposed approaches are evaluated with some numerical study where we consider a ULA having $N = 40$ antennas with half wavelength spacing as our underlying array. The sources are generally considered to be correlated

while spatially and temporally white noise is assumed with a signal to noise ratio (SNR) of 0 dB. Note that each signal coming from different sources is assumed to have equal power and the SNR is defined with respect to the power of each signal.

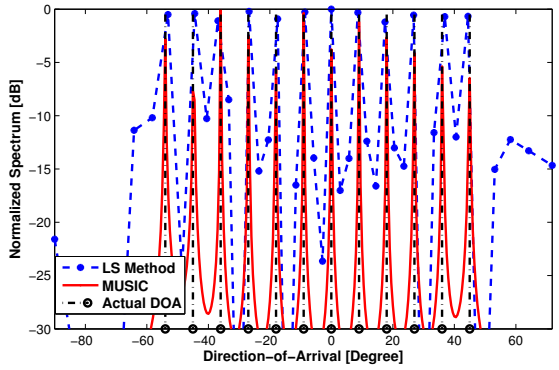

Fig. 2. Normalized spectrum (in dB) of both LS and MUSIC approaches versus DOA (degree) for the first experiment with $K = 12$ correlated sources, SNR = 0 dB, $Q = N = 40$, $L = 28$ and $M = 10$.

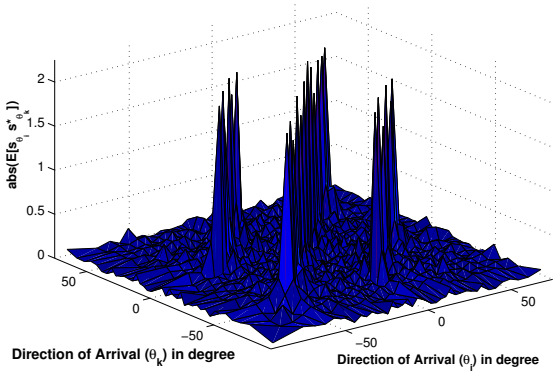

Fig. 3. The magnitude of the elements of the estimated correlation matrix $\hat{\mathbf{R}}_{\tilde{s}}$ computed using LS for the first experiment. Here $K = 12$, SNR = 0 dB, $Q = N = 40$, $L = 28$ and $M = 10$.

In the first experiment, we set the number of time slots per scanning period L to $L = 28$. Ideally, the selection of the activated antennas in all time slots should minimize the number of active antennas per time slot M. According to (17), the lower bound for M in this scenario is given by $M \geq 8$. However, we employ the proposed algorithm provided in Table II in order to obtain a sub-optimal solution for M and $\{\Gamma_l\}_{l=0}^{27}$, which contain the active antenna indices for each time slot. Running the algorithm in Table II for $N = 40$ and $L = 28$ results in $M = 10$ (which is larger than the lower bound) and produces the indices of the 10 antennas to be activated in each of the 28 time slots. This antenna array setup produces a full column rank 2800×1600 matrix $\mathbf{\Psi}$ in (11). In order to simulate the case where the number of sources is more than the number of active antennas per time slot M, we generate $K = 12$ sources with 9 degrees of separation, i.e., $\{\theta_k\}_{k=1}^{12} = \{-54^0, -45^0, \ldots, 45^0\}$. In addition, we also set the signal that comes from angle θ_k to be exactly the same as the one coming from direction θ_{k+6} in order to investigate the performance of the proposed approaches for correlated sources. This leads to six pairs of fully correlated sources. The total number of time samples per time slot and the total number of scanning periods are set to $S = 1$ and $P = 57$, respectively, leading to a total number of time samples per active antenna of $PSL = 1596$. In this first experiment, both the LS approach of Section III-A and the MUSIC approach of Section III-C are examined. For the LS approach, the full column rank condition of $\tilde{\mathbf{A}}$ (and thus $\tilde{\mathbf{A}}^* \otimes \tilde{\mathbf{A}}$) in (18) is satisfied by setting the set of investigated angles $\{\tilde{\theta}_q\}_{q=1}^{40}$ according to (19) with $Q = 40$. Here, the diagonal of $\hat{\mathbf{R}}_{\tilde{s}}$ in (18) recovered using LS gives the received power at $\{\tilde{\theta}_q\}_{q=1}^{40}$ and is illustrated in Fig. 2. Note that the actual angles of arrival are also plotted as vertical lines for simplicity. It is clearly shown that the 12 correlated sources can be detected using LS although the DOA estimates produced by LS do not exactly coincide with the actual DOAs. For the MUSIC approach, the spatial smoothing process is performed by setting the number of overlapping subarrays N_s to $N_s = 20$ and the number of antennas per subarray N_a to $N_a = 21$. The resulting MUSIC estimate is also plotted in Fig. 2 and it generally outperforms the LS estimate. However, it should be noted that the LS method does not require spatial smoothing. Fig. 3 illustrates the LS estimate of the magnitude of the correlation between the incident signals at different investigated angles $\tilde{\theta}_q$ for this first scenario. Observe how both the power of the 12 sources (indicated by the diagonal of $\hat{\mathbf{R}}_{\tilde{s}}$) and the magnitude of the cross-correlation between the sources are well-identified.

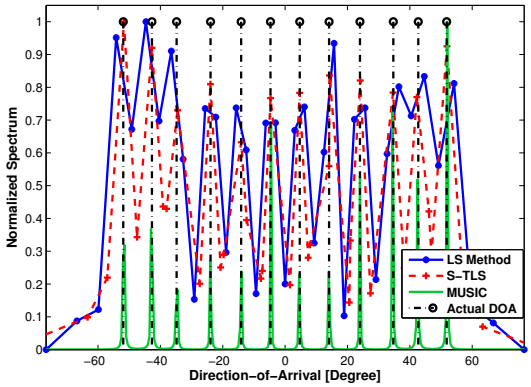

Fig. 4. Normalized spectrum (in normal scale) of LS, S-TLS and MUSIC approaches versus DOA (degree) for the second experiment with $K = 12$ correlated sources, SNR = 0 dB, $Q = 37$, $N = 40$, $L = 28$ and $M = 10$.

In the second experiment, we examine the impact of a grid mismatch on the performance of the LS approach by setting the actual angles of arrival $\{\theta_k\}_{k=1}^{12}$ to directions that are sufficiently different from the defined grid points, that is $\{\theta_k\}_{k=1}^{12} = \{-51.9^0, -42.7^0, -34.8^0, -23.9^0, -14.1^0, -4.7^0, 4.7^0, 14.1^0, 24^0, 34.7^0, 42.7^0, 51.8^0\}$. Here, we use the same dynamic array configuration as the one used in the first experiment (i.e., $N = 40$, $M = 10$, $L = 28$, $P = 57$ and $S = 1$). We also investigate the performance of the S-TLS approach of Section III-B and the MUSIC approach of Section III-C. The number of investigated angles that are

defined for the LS approach is $Q = 37$ where $\{\tilde{\theta}_q\}_{q=1}^{37}$ is defined according to (19). The performance of the S-TLS approach is evaluated by executing the algorithm given by Table III and using the initial investigated angles $\{\tilde{\theta}_q\}_{q=1}^{37}$ that are used by the LS approach. Here, the maximum number of iterations in Table III is set to 110 while ϵ is equal to 10^{-3}. Fig. 4 provides the normalized spectrum (in linear scale) for the second experiment. Again, the actual angles of arrival are also plotted as vertical lines and they are given a normalized spectrum of 1 for simplicity. We can see from Fig. 4 that the quality of the LS estimate slightly deteriorates whereas that of the MUSIC estimate remains acceptable. As we can also see here, the corrected grid of the S-TLS approach can generally match the actual angles of arrival and the 12 correlated sources can generally be detected by the S-TLS approach. Meanwhile, Fig. 5 illustrates the LS estimate (top part) and the S-TLS estimate (bottom part) of the magnitude of the correlation between the incident signals at different investigated angles for the second experiment. While the power of the 12 sources (given by the diagonal of $\hat{\mathbf{R}}_{\tilde{s}}$) and the magnitude of the cross-correlation between the sources can be identified by the LS approach, the peak values are not as clear as the ones found for the first experiment. On the other hand, clear peak values that indicate both the power of the 12 sources and the magnitude of the cross-correlation between the sources are found in the S-TLS estimate.

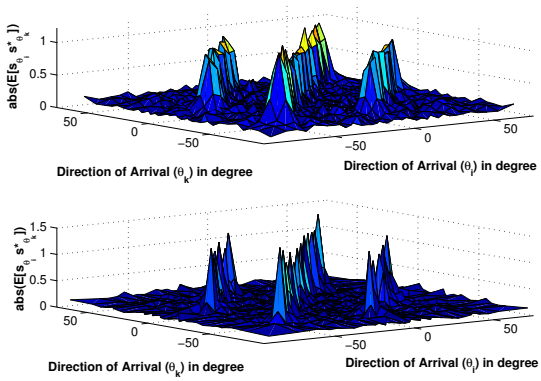

Fig. 5. The magnitude of the elements of the estimated correlation matrices $\hat{\mathbf{R}}_{\tilde{s}}$ computed using LS (top part) and $\hat{\mathbf{R}}_{\tilde{s}}$ computed using S-TLS (bottom part) for the second experiment. Here $K = 12$, SNR = 0 dB, $Q = 37$, $N = 40$, $L = 28$ and $M = 10$.

V. Conclusion

In this paper, a new second-order statistics based DOA estimation approach for possibly coherent sources is proposed by adopting a dynamic linear array, which is developed by performing a periodic scanning of an underlying ULA having N antennas. In different time slots of a scanning period, we activate a different set of M antennas. We collect the spatial correlation matrices of the output of the arrays of active antennas for all time slots and present them as a linear function of the correlation matrix of the incident signals at the predefined angular grid of investigated angles. We also present the theoretical condition that needs to be satisfied in order to ensure the full-rank condition of the system matrix. This allows us to first reconstruct the spatial correlation matrix $\mathbf{R}_x$ using LS. Next, we can estimate the correlation matrix of the incident signals at the investigated angles using LS as well. However, since the latter LS DOA estimation approach is vulnerable to the so-called grid mismatch effect, we also propose S-TLS to reconstruct the correlation matrix of the incident signals at an optimally perturbed angular grid of investigated angles from the reconstructed $\mathbf{R}_x$. Another possible option is to apply spatial smoothing and MUSIC on the reconstructed $\mathbf{R}_x$. The simulation study has indicated how our dynamic array approach provides many possible alternatives for different scenarios and it generally performs satisfactory even when the number of correlated sources is larger than the number of active antennas at each time slot. Hence, the proposed method can be considered as one possible candidate for DOA estimation in case of more correlated sources than active sensors.

References

[1] T.J. Shan, M. Wax, and T. Kailath, "On spatial smoothing for direction-of-arrival estimation of coherent signals," *IEEE Transactions on Acoustics, Speech, and Signal Processing*, vol. 33, no. 4, pp. 806-811, August 1985.

[2] R.O. Schmidt, "Multiple emitter location and signal parameter estimation,"*IEEE Transactions on Antennas and Propagation*, vol. 34, no. 3, pp. 276-280, March 1986.

[3] A.J. Barabell, "Improving the resolution performance of eigenstructure-based direction-finding algorithm," *Proc. of IEEE International Conference on Acoustics, Speech, and Signal Processing*, Boston, Massachusetts, pp. 336-339, April 1983.

[4] J.A. Cadzow, "A high resolution direction-of-arrival algorithm for narrow-band coherent and incoherent sources," *IEEE Transactions on Acoustics, Speech, and Signal Processing*, vol. 36, no. 7, pp. 965-979, July 1988.

[5] D. Malioutov, M. Cetin, and A.S. Willsky, "A sparse signal reconstruction perspective for source localization with sensor arrays,"*IEEE Transactions on Signal Processing*, vol. 53, no. 8, pp. 3010-3022, August 2005.

[6] M.M. Hayder and K. Mahata, "Direction-of-arrival estimation using a mixed $\ell_{2,0}$ norm approximation," *IEEE Transactions on Signal Processing*, vol. 58, no. 9, pp. 4646-4655, September 2010.

[7] J. Yin and T. Chen, "Direction-of-arrival estimation using a sparse representation of array covariance vectors," *IEEE Transactions on Signal Processing*, vol. 59, no. 9, pp. 4489-4493, September 2011.

[8] W. Ma, T. Hsieh, and C. Chi, "DOA estimation of quasi-stationary signals via Khatri-Rao subspace," *Proc. of IEEE International Conference on Acoustics, Speech, and Signal Processing*, Taipei, Taiwan, pp. 2165-2168, April 2009.

[9] P. Pal and P.P. Vaidyanathan, "Nested arrays: a novel approach to array processing with enhanced degrees of freedom,"*IEEE Transactions on Signal Processing*, vol. 58, no. 8, pp. 4167-4181, August 2010.

[10] P. Pal and P.P. Vaidyanathan, "Coprime sampling and the MUSIC algorithm," *Proc. of IEEE Digital Signal Processing and Signal Processing Education Workshop*, Sedona, Arizona, pp. 289-294, January 2011.

[11] P. Pal and P.P. Vaidyanathan, "Sparse sensing with co-prime samplers and arrays,"*IEEE Transactions on Signal Processing*, vol. 59, no. 2, pp. 573-586, February 2011.

[12] S. Shakeri, D.D. Arianandа, and G. Leus, "Direction of arrival estimation using sparse ruler array design," *Proc. of The 13th IEEE International Workshop on Signal Processing Advances in Wireless Communications*, Cesme, Turkey, June 2012.

[13] P. Pal and P.P. Vaidyanathan, "Correlation-aware techniques for sparse support recovery," *Proc. of IEEE Statistical Signal Processing (SSP) Workshop*, Ann Arbor, Michigan, pp. 53-56, August 2012.

[14] E. Gonen, M.C. Dogan, and J.M. Mendel, "Applications of cumulants to array processing: direction-finding in coherent signal environment," *Proc. of The 28-th Asilomar Conference on Signal, Systems and Computers*, Pacific Grove, California, pp. 633-637, November 1994.

[15] H. Zhu, G. Leus, and G. Giannakis, "Sparsity-cognizant total least-squares for perturbed compressive sampling,"*IEEE Transactions on Signal Processing*, vol. 59, no. 5, pp. 2002-2016, May 2011.